J Mol Neurosci (2016) 60:21–32
DOI 10.1007/s12031-016-0758-z

Gastrodin Protects Neural Progenitor Cells Against Amyloid β (1–42)-Induced Neurotoxicity and Improves Hippocampal Neurogenesis in Amyloid β (1–42)-Injected Mice

Meng Li[1] · **Sumin Qian**[2]

Received: 26 February 2016 / Accepted: 11 April 2016 / Published online: 26 April 2016

Abstract The aim of this study was to investigate the neuroprotective effects of gastrodin (GAS), one of the major bioactive components of *Gastrodia elata* Blume (Tian Ma), against amyloid β (Aβ) (1–42)-induced neurotoxicity in primary neural progenitor cells (NPCs). We found that pretreatment with GAS not only prevents a loss in cell viability following treatment with Aβ (1–42) but also counteracts Aβ (1–42)-triggered release of pro-inflammatory cytokines and nitric oxide (NO) in a dose-dependent manner. Additionally, GAS was able to attenuate Aβ (1–42)-induced apoptosis in NPCs, evidenced by the decreased percentage of apoptotic cells and altered expression of apoptosis-related proteins in response to GAS pretreatment prior to Aβ (1–42) exposure. Furthermore, in Aβ (1–42)-injected C57BL/6 mice, we found that systemic administration of GAS could improve hippocampal neurogenesis, manifested by the increased number of SOX-2 and doublecortin (DCX)-positive cells in the DG area. Mechanistic studies revealed that in NPCs, GAS could reverse the Aβ (1–42)-induced increase in phosphorylation of MEK-1/2, extracellular signal-regulated kinases (ERK), and c-Jun N-terminal kinase (JNK). When combining GAS with the MEK inhibitor U0126 or the JNK inhibitor SP600125, we observed a synergistic effect against Aβ (1–42)-induced reduction in cell viability of NPCs. Taken together, these results show the efficacy and underlying mechanism of GAS against amyloid β (1–42)-induced neurotoxicity and provide substantial insight into the potential merits of GAS for its clinical application in the treatment of Alzheimer's disease.

Keywords Gastrodin · Neural progenitor cells · Amyloid β (1–42) · Hippocampal neurogenesis

Introduction

Currently, Alzheimer's disease (AD) is the most common form of dementia among the elderly, affecting an estimated population of over 40 million worldwide (Burns and Iliffe 2009). At the histological level, AD is characterized by senile plaques and neurofibrillary tangles, which refer to extracellular aggregates composed by amyloid peptide (Aβ), and intracellular aggregates composed by hyperphosphorylated forms of tau protein, respectively (Thal et al. 2015). In recent years, it has been well documented that the accumulation of Aβ into senile plaques elicits a pathogenic cascade in the brain, including altered neuronal activity, synaptic deficits, oxidative stress, and inflammatory responses (Dawkins and Small 2014). Of these pathogenic processes, chronic inflammatory responses are considered a key feature of AD, which has been evidenced by the fact that in AD patients, the brain usually has the signs of inflammation and shows increased expression of several pro-inflammatory cytokines that are hardly observed in normal brains (Minter et al. 2016). Under the inflammatory environment, neuronal apoptosis occurs, consequently inducing the progressive loss of neurons and ultimately causing cognitive and motor impairments (Fuster-Matanzo et al. 2013).

Electronic supplementary material The online version of this article (doi:10.1007/s12031-016-0758-z) contains supplementary material, which is available to authorized users.

✉ Meng Li
dr.limeng@outlook.com

[1] Fifth Department of Neurology, Cangzhou Central Hospital, No. 16 Xinhua Western Road, Cangzhou, Hebei Province 061000, China

[2] Second Department of Gynecology, Cangzhou Central Hospital, No. 16 Xinhua Western Road, Cangzhou, Hebei Province 061000, China

In recent years, formation of new neurons, i.e., neurogenesis, has been demonstrated in the normal adult human brain (Eriksson et al. 1998). Adult neurogenesis occurs principally in two brain regions: the subventricular zone (SVZ) and the subgranular zone (SGZ) of the hippocampus, where neural progenitor cells (NPCs) are concentrated and involved in this process (Zhao et al. 2008). In the adult SGZ, NPCs generate intermediate progenitors, which subsequently migrate a short distance into the granule cell layer of the dentate gyrus (DG) of the hippocampus and differentiate into new neurons (Martino et al. 2014). In AD brains, however, Aβ-induced neurotoxicity (e.g., inflammatory responses, apoptosis, and oxidative stress) has been found to have remarkable influence on proliferation, survival, and differentiation and fate determination of NPCs, thus greatly impairing adult neurogenesis (Winner and Winkler 2015). Hence, counteracting Aβ-induced neurotoxicity and restoring neurogenesis from NPCs could be a beneficial strategy not only for endogenous neural repair but for improving the deficits directly provoked by AD.

To date, researchers have been concentrated on the development of anti-inflammatory medications as a treatment option for patients with AD (Wang et al. 2015a). Chemically synthesized drugs such as the nonsteroidal anti-inflammatory drugs (NSAIDs) and glucocorticoid steroids have been well studied. Nevertheless, in spite of strong anti-inflammatory activities, none of these drugs can facilitate neurogenesis in vitro or in vivo (Apetz et al. 2014). Therefore, more and more researchers have focused their attention on natural products, which can be potential sources of new chemical entities (NCEs) with both anti-inflammatory and neurogenesis-promoting effects.

Gastrodin (GAS) is one of the major bioactive components of *Gastrodia elata* Blume (Tian Ma) (Fig. 1), a Chinese traditional herbal medicine that is widely used for the treatment of headache, convulsions, hypertension, and cardiovascular diseases (Jang et al. 2015). Recent studies have demonstrated the anti-inflammatory of GAS both in vitro and in vivo (Qu et al. 2015; Yang et al. 2013). Regarding the neuroprotective activities of GAS, Hu et al. (2014) reported that GAS is able to alleviate memory deficits and significantly attenuate Aβ deposition and glial activation in a mouse model of AD. Another in vivo study demonstrated that GAS suppresses the Aβ-induced increase of spontaneous discharge in the entorhinal cortex of rats (Chen et al. 2014). More importantly, Sun et al. (2012) found that GAS induces neural stem cell differentiation into neurons, while in rats, systemic administration of GAS upregulates proliferation of hippocampal-derived neural stem cells (Wang et al. 2014). Despite of these encouraging findings, few studies have reported the protective effects of GAS against Aβ-induced neurotoxicity in NPCs. Whether GAS can improve Aβ-mediated impairment of hippocampal neurogenesis is also poorly understood. In this study, therefore, we used mouse primary NPCs and Aβ-injected mice to explore the neuroprotective and neurogenesis-promoting activities of GAS. The underlying molecular mechanism was also investigated.

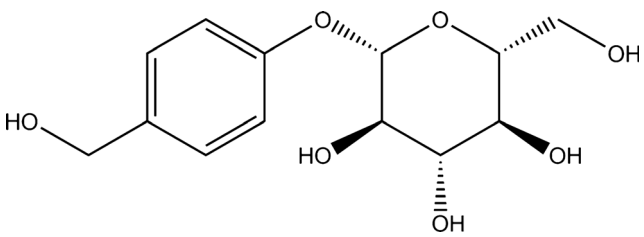

Fig. 1 Molecular structure of GAS

Materials and Methods

Reagents and Animals

GAS (purity >99 %) was purchased from Chongqing Kangheyuecheng Pharmaceutical Technology Co., Ltd. (Chongqing, China). Synthetic Aβ (1–42), SP600125, and U0126 were purchased from Sigma-Aldrich China (Shanghai, China). Cell counting kit-8 (CCK-8) was provided by Dojindo Laboratories (Kumamoto, Japan). The ApoDETECT Annexin V-fluorescein isothiocyanate (FITC) apoptosis detection kit, the nitric oxide (NO) assay kit, and the enzyme-linked immunosorbent assay (ELISA) kits for human tumor necrosis factor alpha (TNF-α), interleukin (IL)-1β, and IL-6 were obtained from ThermoFisher Scientific Inc. (Waltham, MA, USA). C57BL/6 mice were from Beijing Laboratory Animal Research Centre (Beijing, China).

Preparation of Oligomeric Aβ (1–42)

Oligomeric Aβ (1–42) was prepared and characterized according to the procedure described previously (Sanphui and Biswas 2013). First, lyophilized Aβ (1–42) was dissolved in 1,1,1,3,3,3 hexafluoro-2-propanol (HFIP, Sigma-Aldrich) to a final concentration of 1 mM. Then, the resulting solution was aliquoted into Eppendorf tubes, and HFIP was evaporated under vacuum. The remaining dried Aβ (1–42) was resuspended in dimethylsulfoxide (DMSO) to generate a stock solution of 5 mM. Afterward, the obtained stock solution was diluted with phosphate-buffered saline (PBS) to a final working concentration of 100 μM. Prior to use, the working solution was incubated at 37 °C for 5 days. The final concentration of Aβ (1–42) and incubation periods in all in vitro experiments were determined based on previous literature (He et al. 2013; Hou et al. 2014; Karkkainen et al. 2014) and a pilot study (Supplementary Figs. 1 and 2).

Culture of Primary NPCs

Primary NPCs were prepared from the hippocampus of 8-week-old C57BL/6 mice and were cultured according to the protocol described in previous literature (Smith et al. 2015). In brief, after removing superficial blood vessels, hippocampus tissues were minced and then digested in Dulbecco's modified Eagle's medium (DMEM) (ThermoFisher Scientific Inc.) supplemented with 250 U/ml DNase I (Worthington Biochemicals, Lakewood, NJ, USA), 2.5 U/ml Papain (Worthington Biochemicals), and 1 U/ml Dispase II (Sigma-Aldrich China) (37 °C, 30 min). After being into single cells, NPCs were purified using a Percoll gradient of 65 % (vol/vol). Then, the purified NPCs were plated on uncoated tissue culture dishes at a density of 10^5 cells/cm^2 and cultured in NeuroBasal A medium (ThermoFisher Scientific Inc.) containing serum-free B27 Supplement Minus Vitamin A (ThermoFisher Scientific Inc.), 2 mM L-glutamine, penicillin-streptomycin (100 U/ml and 100 mg/ml, respectively), 20 ng/ml basic fibroblast growth factor (bFGF), and 20 ng/ml epidermal growth factors (EGF). After being cultured for 48 h, NPCs were dissociated using cell dissociation kit (Sigma-Aldrich, China). Then, the dissociated cells were resuspended in proliferation medium and seeded into 96-well plates at a density of 10^3 cells per well for subsequent experiments.

Cell Viability Assay

CCK-8 was used to determine cell viability under different treatment conditions. In brief, NPCs were seeded into 96-well plates at a density of 10^3 cells per well. Before being exposed to 10 μM Aβ (1–42) for 48 or 96 h, cells were pretreated with varying concentrations of GAS (0, 5, 20, and 50 μg/ml) for 6 h. The concentrations of GAS were chosen according to previous studies (Wang et al. 2014). After exposure to Aβ (1–42) for indicated time periods, CCK-8 reagent was added to each well and incubated at 37 °C for 1 h. Absorbance was measured at 450 nm in a spectrophotometer (Model 680, Bio-Rad, Hercules, CA, USA). Each experiment was performed in sextuplicate and repeated three times.

Analysis of Neurosphere Size and Number

Analysis of neurosphere size and number was used to further validate the neuroprotective effects of GAS. Briefly, NPCs were treated with 10 μM Aβ (1–42) for 96 h, following preincubation with varying concentrations of GAS for 6 h. Then, cells were observed and photographed using a microscope (Olympus 7903, Olympus Inc., Tokyo, Japan). For each experimental group, neurosphere size analysis was performed in 100 randomly selected neurospheres from 10 random fields of view (200×), whereas neurosphere number analysis was performed by calculating the mean neurosphere number of 10 randomly selected 100× fields of view. All analyses were carried out using ImageJ software (version 1.46, http://imagej.nih.gov/ij/).

Measurement of Cytokine and NO Concentrations

Production of TNF-α, IL-1β, and IL-6, as well as NO in primary NPCs was measured using the ELISA or colorimetric kits (ThermoFisher Scientific Inc.). Briefly, after collecting the supernatants of NPCs exposed to different treatment conditions, the concentrations of the three cytokines and NO were detected by the respective kits according to the manufacturer's instructions. All experiments were conducted three times independently.

Quantitative Real-Time Polymerase Chain Reaction

After exposure to various treatments, total RNA was extracted from NPCs using the TRIzol® Plus RNA Purification Kit (ThermoFisher Scientific Inc.) following the manufacturer's instruction. The cDNAs were synthesized using the QuantiTect Reverse Transcription Kit (Qiagen, Hilden, Germany). The primers were synthesized according to previous literature (Wu et al. 2003). Quantitative real-time PCR (qRT-PCR) was carried out using an iQ5™ RT-PCR System with iQ™ SYBR® Green Supermix kit (Bio-Rad). Messenger RNA (mRNA) levels were calculated using the delta-delta cycle threshold (ΔΔCt) method (Schmittgen and Livak, 2008). Glyceraldehyde-3-phosphate dehydrogenase (GAPDH) served as an internal control. All experiments were conducted three times independently.

Western Blot

Primary NPCs exposed to various treatments were harvested by centrifugation. Afterward, cells were lysed using RIPA buffer. The obtained homogenates were centrifuged at 10,000*g* for 10 min to remove debris. The supernatant was then subject to protein concentration assay and Western blot analysis according to routine procedures. Immunoblots were carried out using the following antibodies: inducible nitric oxide synthase (iNOS) (NB300–605) (1:500, Novus Biologicals, Littleton, CO, USA); cyclooxygenase-2 (COX-2) (ab52237) and cleaved caspase 3 (p17 fragment, ab2302) (1:1000, Abcam, Cambridge, UK); Bcl-2 (#2876), Bcl-XL (#2762), Bax (#2772), MEK-1/2 (#9122), and phosphorylated MEK-1/2 at serine 217/221 (p-MEK-1/2, #9121) (1:500, Cell Signaling, Danvers, MA, USA); ERK (sc-94), JNK (sc-7345), p38 (sc-535), phosphorylated ERK at threonine 202/tyrosine 204 (p-ERK, sc-16982), phosphorylated JNK at threonine 183/tyrosine 185 (p-JNK, sc-12882), and phosphorylated p38 at tyrosine 182 (p-p38, sc-7973) (1:500, Santa Cruz

Biotechnology, Dallas, TX, USA). The antibody against β-actin (A2228, Sigma-Aldrich China) served as loading control. All immunoblots were developed using an enhanced chemiluminescence (ECL) Western blotting detection kit (ThermoFisher Scientific Inc.) and then quantified using ImageJ software. All experiments were conducted three times independently.

Annexin V Assay

Quantification of apoptotic NPCs was performed using an Annexin V-FITC apoptosis detection kit (ThermoFisher Scientific Inc.) according to the manufacturer's instruction. Briefly, 1.0×10^5 NPCs under various treatment conditions were harvested. After being washed with cold PBS, cells were resuspended in 500 μl of Annexin V binding buffer. Then, 5 μl of Annexin V-FITC and 5 μl of propidium iodide (PI) were added. After incubation in the dark for 15 min at room temperature, the percentage of Annexin V-positive NPCs was quantified using a flow cytometer (FACScan Flow Cytometry System; BD Bioscience, San Jose, CA, USA). All experiments were conducted three times independently.

Aβ (1–42)-Injected Mice Model and GAS Treatment

Twenty-four 8-week-old male C57BL/6 mice were divided into four groups: sham-operated group (sham, $n = 6$), sham-treated with 60 mg/kg GAS group (60 mg/kg GAS, $n = 6$), Aβ (1–42)-injected group (Aβ (1–42), $n = 6$), and GAS treatment group (Aβ (1–42) + 60 mg/kg GAS, $n = 6$). Before the study, all mice were housed under a 12-h light-dark cycle and had free access to food and water. All animal handling procedures were conducted in accordance with institutional guidelines. The protocol of animal study was approved by the Animal Ethics Committee of Cangzhou Central Hospital.

The administration of Aβ (1–42) oligomers was performed according to a previously described protocol with minor modifications (Zhao et al. 2013). Briefly, C57BL/6 mice were positioned in a stereotaxic frame and anesthetized with 2 % isoflurane in 100 % oxygen via a nose cone. Four microliters of Aβ (1–42) oligomer saline solution (1 μg/μl) were injected into the bilateral hippocampi by infusion cannulae. For animals in the GAS treatment group, 60 mg/kg GAS (dissolved in sterile saline) was administered intraperitoneally (i.p.) once daily for 15 consecutive days, in addition to infusion of Aβ (1–42) oligomers. The dosage and frequency of GAS administration were based on previous literature (Wang et al. 2014; Zhao et al. 2012). The two sham groups were treated either with vehicle (saline) or with vehicle plus GAS (i.p. 60 mg/kg, once daily for 15 days).

Immunohistochemistry

Tissue processing and immunohistochemistry (IHC) were carried out following routine protocols. In brief, mice were anesthetized with isoflurane and transcardially perfused with 0.9 % saline. Brains were removed, fixed in phosphate-buffered 4 % paraformaldehyde (pH 7.4), and then sectioned coronally at 40 μm using a cryomicrotome (Leica, Wetzlar, Germany). The obtained sections were treated with 10 mM sodium citrate for 30 min at 90 °C. After being washed with Tris-buffered saline with Tween (TBST), the sections were blocked in 10 % goat serum for 1 h and then incubated with anti-SOX2 (1: 1000, ab97959, Abcam) or anti-doublecortin (DCX) (1: 500, sc-8066, Santa Cruz Biotechnology) overnight at 4 °C. Immunopositive cells were quantified using ImageJ software. The total number of immunopositive cells per DG was estimated according to the method reported by Smith et al. (2015).

Statistical Analysis

All statistical analyses were carried out in GraphPad Prism 6.01 software (GraphPad Software, La Jolla, CA, USA). The D'Agostino-Pearson omnibus normality test was used to test the normality of data. Data with normal distribution are presented as mean ± standard deviation (SD) or mean ± standard error of the mean (SEM), while data with skewed distribution are presented as median and range (minimum and maximum). One-way analysis of variance (ANOVA) with Tukey post hoc test (for multiple comparisons) was used to compare means among groups, whereas the Kruskal-Wallis test with Dunn's post hoc test was used to compare medians among groups. A P value less than 0.05 was considered statistically significant.

Results

GAS Protects NPCs Against Aβ (1–42)-Induced Neurotoxicity

First, we examined the effects of GAS on NPC viability. As shown in Fig. 2a, treatment with up to 50 μg/ml of GAS for 48 or 96 h did not influence cell viability of NPCs. Then, we investigated the protective effects of GAS against Aβ (1–42)-induced neurotoxicity in NPCs. As indicated in Fig. 2b, NPCs exposed to 10 μM oligomeric Aβ (1–42) for 48 and 96 h showed a significant decrease in cell viability as compared to vehicle-treated controls. When NPCs were incubated with varying doses of GAS for 6 h prior to Aβ (1–42) treatment, the Aβ (1–42)-induced loss of cell viability was markedly attenuated in a dose-dependent manner, and 50 μg/ml GAS displayed the most potent effect among the doses investigated.

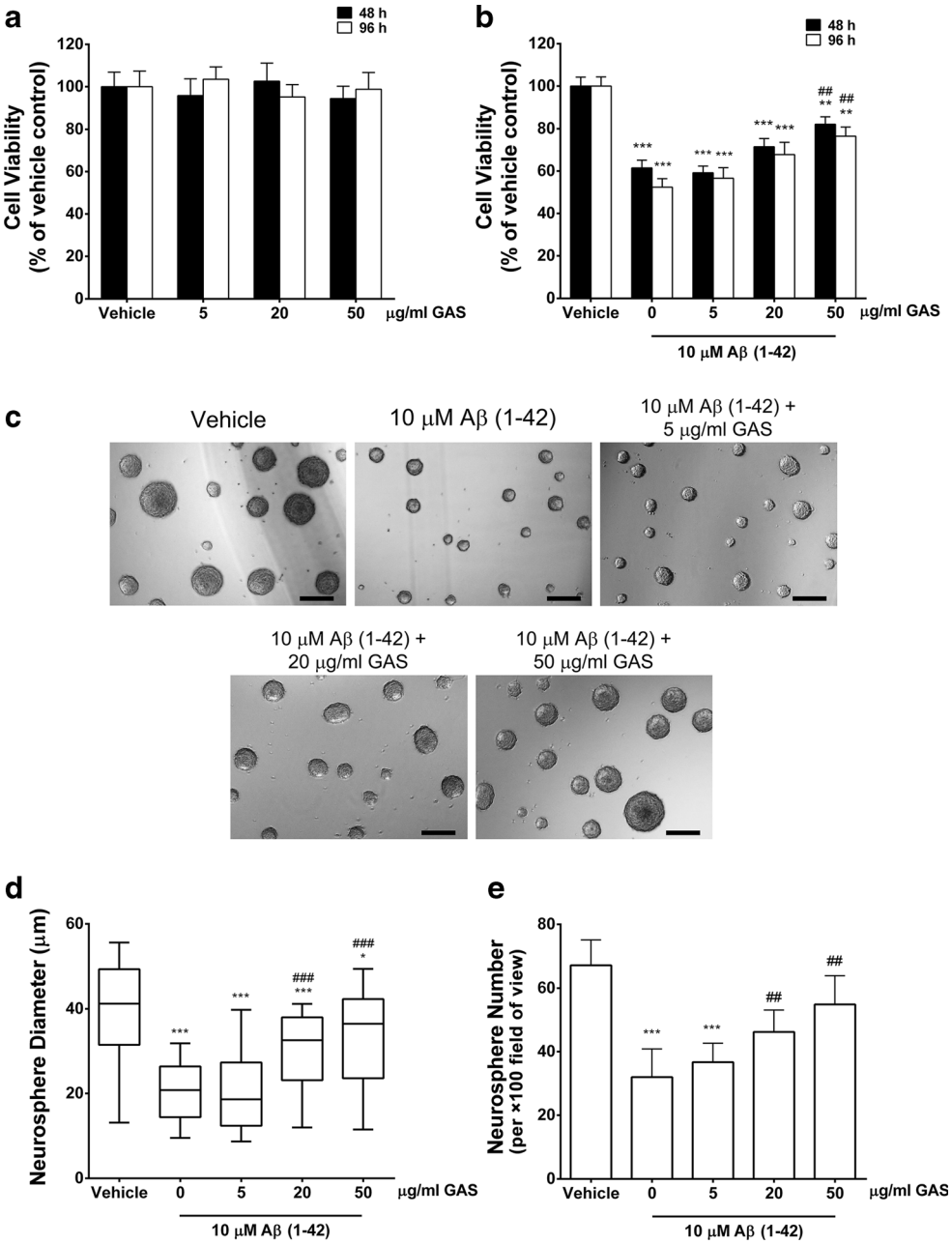

Fig. 2 GAS protects NPCs against Aβ (1–42)-induced neurotoxicity. **a** Treatment with up to 50 μg/ml of GAS for 48 or 96 h did not influence cell viability of NPCs. **b** NPCs exposed to 10 μM oligomeric Aβ (1–42) for 48 and 96 h showed a significant decrease in cell viability, while this Aβ (1–42)-induced cell viability loss was markedly attenuated by preincubation with GAS. **c** The morphological appearances of NPCs after the indicated treatments for 96 h (*scale bar* = 50 μm). **d**, **e** Analysis of neurosphere size and number after the indicated treatments for 96 h. Cell viability assay was performed in sextuplicate using CCK-8 kit and repeated three times, and the results are presented as mean ± SEM. Neurosphere size analysis was performed in 100 randomly selected neurospheres from 10 random fields of view (200×), and the results are presented as median (*middle line*) and range (*outer lines*). Neurosphere number analysis was performed by calculating the mean neurosphere number of 10 randomly selected 100× fields of view, and the results are presented as mean ± SD. $^{**}P < 0.01$ and $^{***}P < 0.001$, as compared with the vehicle group; $^{\#\#}P < 0.01$ and $^{\#\#\#}P < 0.001$, as compared with the group treated with Aβ (1–42) alone

Next, we validated the protective effects of GAS based on morphological features of NPCs. The morphological appearances of NPCs after the indicated treatments for 96 h, as well as the quantification of neurosphere size, are presented in Fig. 2c, 2d. Cells exposed to 10 μM Aβ (1–42) generated significantly smaller neurospheres compared with those treated with vehicle, indicating that the cell proliferation was suppressed by Aβ (1–42). Nevertheless, this suppressive effect could be counteracted by preincubation with GAS dose-independently. In addition, as shown in Fig. 2e, Aβ (1–42)-treated NPCs formed remarkably fewer neurospheres than the vehicle-treated cells did. When NPCs were pretreated with varying concentrations of GAS, the impact of Aβ (1–42) on neurosphere formation was attenuated with an increase of GAS concentration. Collectively, these results demonstrate the protective activities of GAS against Aβ (1–42)-induced neurotoxicity in NPCs.

GAS Counteracts the Release of Pro-Inflammatory Cytokines and Nitric Oxide Induced by Aβ (1–42)

It has been well documented that Aβ is able to trigger inflammatory responses, which can promote its neurotoxicity (Fuster-Matanzo et al., 2013). Therefore, we investigated whether GAS has anti-inflammatory effects on Aβ (1–42)-treated NPCs. As depicted in Fig. 3a, the production of

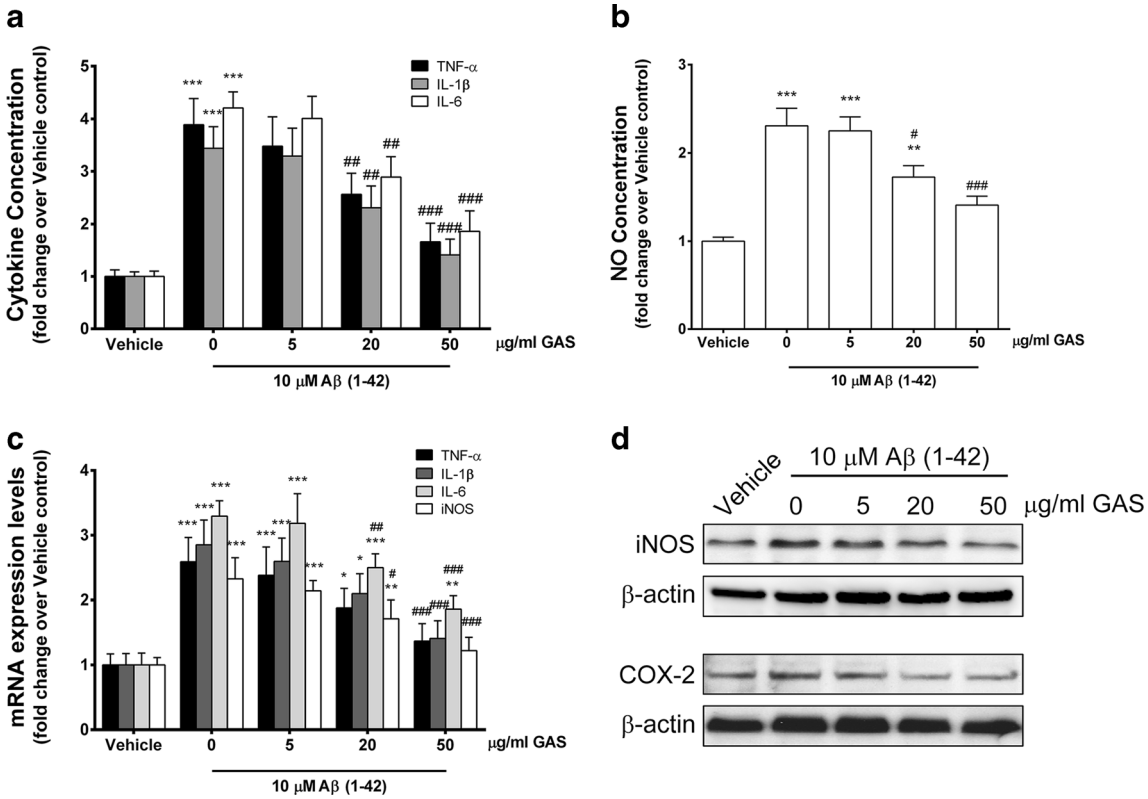

Fig. 3 GAS counteracts the release of pro-inflammatory cytokines and NO induced by Aβ (1–42). NPCs were incubated with different doses of GAS for 6 h before exposure to 10 μM oligomeric Aβ (1–42) for an additional 96 h. **a** The production of TNF-α, IL-1β, and IL-6 was measured by the correpsonding ELISA kits. **b** The production of NO was assayed by a colorimetric kit. **c** qRT-PCR analysis of mRNA levels of TNF-α, IL-1β, IL-6, and iNOS. **d** Expression levels of iNOS and COX-2 detected by Western blot. All data were from three independent experiments and are presented as mean ± SD. $^{*}P < 0.05$, $^{**}P < 0.01$, and $^{***}P < 0.001$, as compared with the vehicle group; $^{\#}P < 0.05$, $^{\#\#}P < 0.01$, and $^{\#\#\#}P < 0.001$, as compared with the group treated with Aβ (1–42) alone

TNF-α, IL-1β, and IL-6 was significantly increased, by 3.9-, 3.4-, and 4.2-fold, in Aβ (1–42)-treated NPCs as compared to those treated with vehicle. When cells were preincubated with GAS, the production of the three cytokines was dramatically suppressed in a dose-dependent manner. In addition, we examined the production of NO, a potent inflammatory mediator, in NPCs upon different treatment. As shown in Fig. 3b, 10 μM Aβ (1–42) induced a considerably higher NO production (2.3-fold) in NPCs than vehicle did. However, this effect could be attenuated by varying doses of GAS, of which 50 μg/ml achieved the most significant reduction in NO production. Taken together, these results revealed that GAS has anti-inflammatory effects against Aβ (1–42)-triggered inflammatory responses in NPCs.

Next, we utilized qRT-PCR to measure the mRNA levels of the three pro-inflammatory cytokines and iNOS, a major enzyme for NO production, under different treatment conditions. In line with the findings presented in Fig. 3a, 3b, exposure to 10 μM Aβ (1–42) significantly increased the mRNA levels of the three cytokines and iNOS in NPCs. When the cells were pretreated with different doses of GAS, a dose-dependent decrease in the mRNA levels was observed for these molecules (Fig. 3c). Additionally, Western blot analysis confirmed that Aβ (1–42) treatment substantially increased the expression of iNOS and COX-2, a well-established marker of inflammation, in NPCs, but this increase could be inhibited by preincubation with GAS dose-dependently (Fig. 3d).

GAS Attenuates NPC Apoptosis Induced by Aβ (1–42)

In order to investigate whether GAS is able to protect NPCs from apoptosis induced by Aβ (1–42), we measured apoptotic events by Annexin V assay and used qRT-PCR and Western blot to analyze the levels of apoptotic markers. As shown in Fig. 4a, NPCs treated with 10 μM Aβ (1–42) for 96 h had 4.5-fold more apoptotic cells than vehicle-treated controls, while NPCs preincubated with GAS showed a dose-dependent decrease in the number of apoptotic cells. qRT-PCR analysis further showed that Aβ (1–42) significantly decreased Bcl-2 and Bcl-XL mRNA levels and increased Bax mRNA level. However, this effect could be counteracted by pretreatment with varying concentrations of GAS (Fig. 4b). Consistent with qRT-PCR data, Western blot analysis also revealed that exposure to Aβ (1–42) could considerably reduce the expression of anti-apoptotic Bcl-2 and Bcl-XL and promote the expression of Bax and cleaved caspase 3 in NPCs. However, these

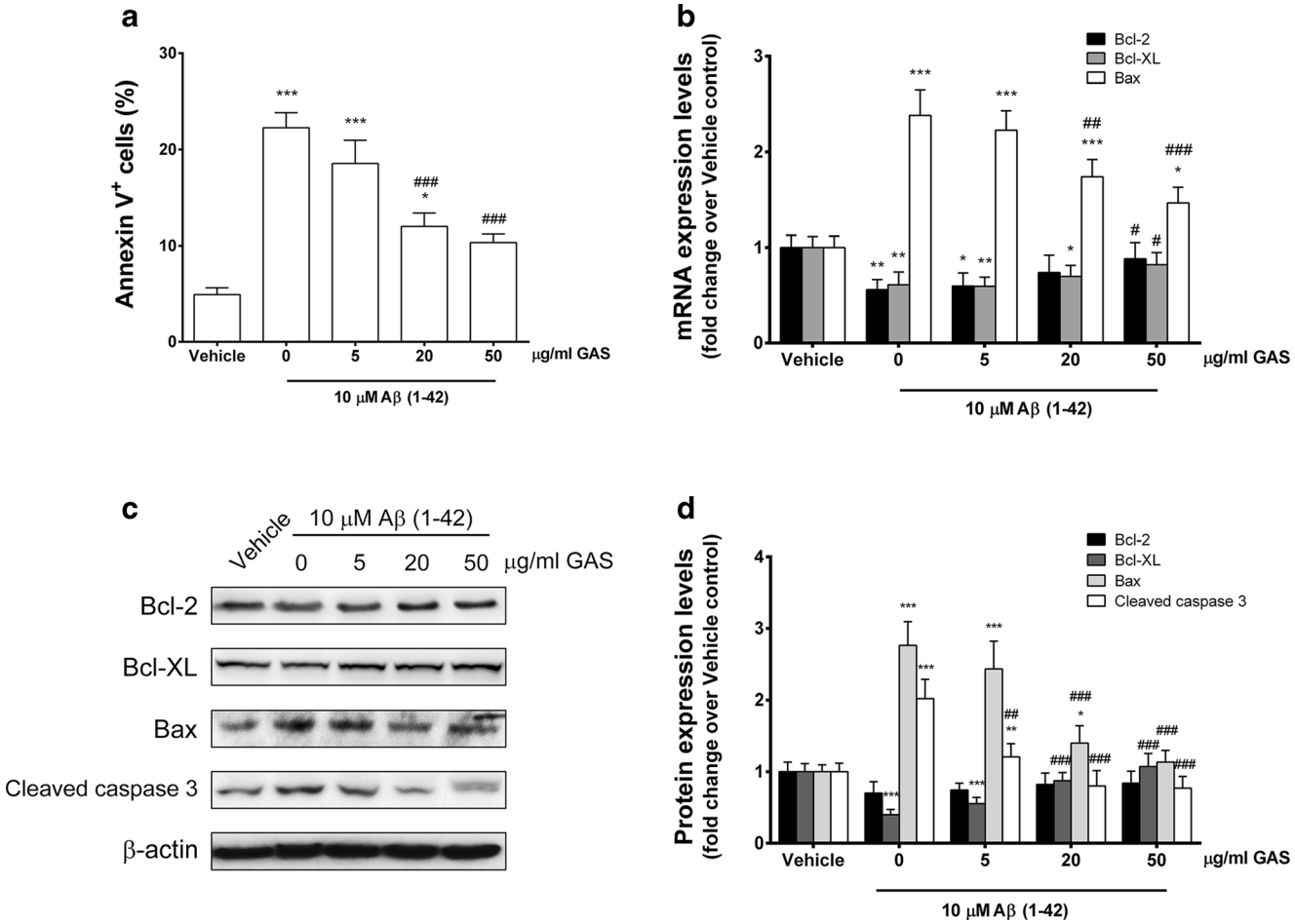

Fig. 4 GAS attenuates NPC apoptosis induced by Aβ (1–42). NPCs were incubated with different doses of GAS for 6 h before exposure to 10 μM oligomeric Aβ (1–42) for an additional 96 h. **a** The percentage of Annexin V-positive cells was analyzed by flow cytometry. **b** qRT-PCR analysis of mRNA levels of Bcl-2, Bcl-XL, and Bax. **c**, **d** Expression levels of Bcl-2, Bcl-XL, Bax, and cleaved caspase 3 were detected by Western blot and quantified with ImageJ software. All data were from three independent experiments and are presented as mean ± SD. $^{*}P < 0.05$, $^{**}P < 0.01$, and $^{***}P < 0.001$, as compared with the vehicle group; $^{\#}P < 0.05$, $^{\#\#}P < 0.01$, and $^{\#\#\#}P < 0.001$, as compared with the group treated with Aβ (1–42) alone

changes could be prevented following preincubation with varying doses of GAS (Fig. 4c, d).

GAS Improves Hippocampal Neurogenesis in Aβ (1–42) -Injected Mice

To further validate the neuroprotective potential in vivo, we administered GAS in Aβ (1–42)-injected C57BL/6 mice and examined its effects on hippocampal neurogenesis. As depicted in Fig. 5a–d, by using IHC analysis, we detected a significant decrease in the number of SOX-2 and DCX-positive cells in the dentate gyrus (DG) of Aβ (1–42)-injected mice, as compared to those treated either with vehicle or with 60 mg/kg GAS alone. However, when mice were administered Aβ (1–42) and GAS simultaneously, this Aβ (1–42)-induced cell number loss could be considerably prevented. Considering SOX-2 and DCX is the marker for neural progenitor cells and differentiated neurons, respectively, these results indicate that GAS is able to improve the impaired hippocampal neurogenesis caused by Aβ (1–42).

GAS Suppresses Aβ (1–42)-Induced Activation of the MAPK Pathway

It has been well documented that the MAPK pathway is highly associated with the neurotoxicity of Aβ (Origlia et al. 2009). Hence, to explore the molecular mechanism underlying the neuroprotective effects of GAS, we treated NPCs with 10 μM Aβ (1–42) in the absence or presence of 50 μg/ml GAS and examined the phosphorylation of several key kinases in the MAPK pathway. As shown in Fig. 6a–d, treatment with Aβ (1–42) led to approximately 2.0-fold increase ($P < 0.001$) in phosphorylation of MEK-1/2, ERK, p38, and JNK in NPCs, as compared to vehicle and GAS alone did. When cells were preincubated with 50 μg/ml GAS, the Aβ (1–42)-induced increase in MEK-1/2, ERK, and JNK

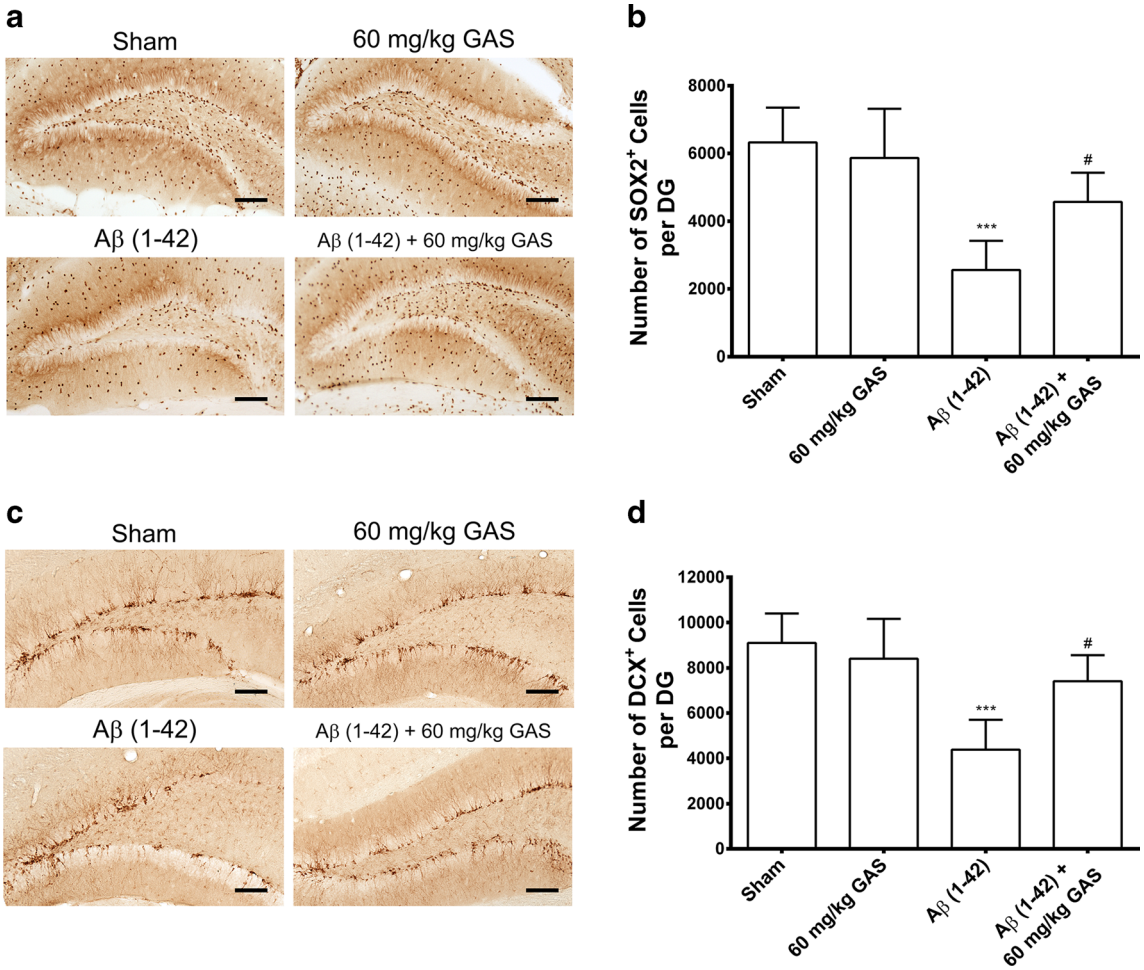

Fig. 5 GAS improves hippocampal neurogenesis in Aβ (1–42)-injected mice. **a**, **b** Representative IHC images of SOX-2 staining and quantification of SOX2-positive cells in the DG area for all treatment groups. **c**, **d** Representative IHC images of DCX staining and quantification of DCX-positive cells in the DG area for all treatment groups. All data were from six animals and are represented as mean ± SD. ***$P < 0.001$, as compared with the sham-operated group; $^{\#}P < 0.05$, as compared with the Aβ (1–42)-injected group

phosphorylation was significantly (MEK-1/2 and ERK) or slightly (JNK) suppressed, but this was not the case for p38. Taken together, these data suggest that GAS potentially inhibits Aβ (1–42)-induced activation of MEK/ERK and JNK signaling cascades.

In order to further verify that the neuroprotective effects of GAS are mediated by the MAPK pathway, we treated NPCs with the MEK inhibitor U0126 (10 μM) or the JNK inhibitor SP600125 (20 μM) for 6 h prior to GAS and Aβ (1–42) treatments. As presented in Fig. 7a, both kinase inhibitors, particularly U0126, could synergistically act with GAS to prevent the Aβ (1–42)-induced decrease in cell viability. Additionally, NPCs pretreated with U0126 and GAS formed significantly larger and more neurospheres compared to those pretreated with GAS alone (Fig. 7b–d). Collectively, these findings suggest that the neuroprotective effects of GAS against Aβ (1–42) in NPCs are most likely mediated by the MAPK pathway.

Discussion

In this study, we report for the first time that GAS can protect mouse primary NPCs from Aβ (1–42)-induced neurotoxicity, which was evidenced by our findings that preincubation with GAS not only prevented a loss in cell viability following treatment with Aβ (1–42), but attenuated Aβ (1–42)-triggered inflammatory responses and cell apoptosis in a dose-dependent manner. Additionally, we found that systemic administration of GAS was able to improve hippocampal neurogenesis in Aβ (1–42)-injected C57BL/6 mice. Mechanistic studies revealed that in NPCs, GAS could counteract Aβ (1–42)-induced activation of MEK/ERK and JNK signaling cascades, thus suggesting that the neuroprotective effects of GAS against Aβ (1–42)-induced toxicity are most likely mediated by the MAPK pathway.

In recent years, accumulating evidence indicates that neurogenesis in the brain of adult mammals occurs throughout

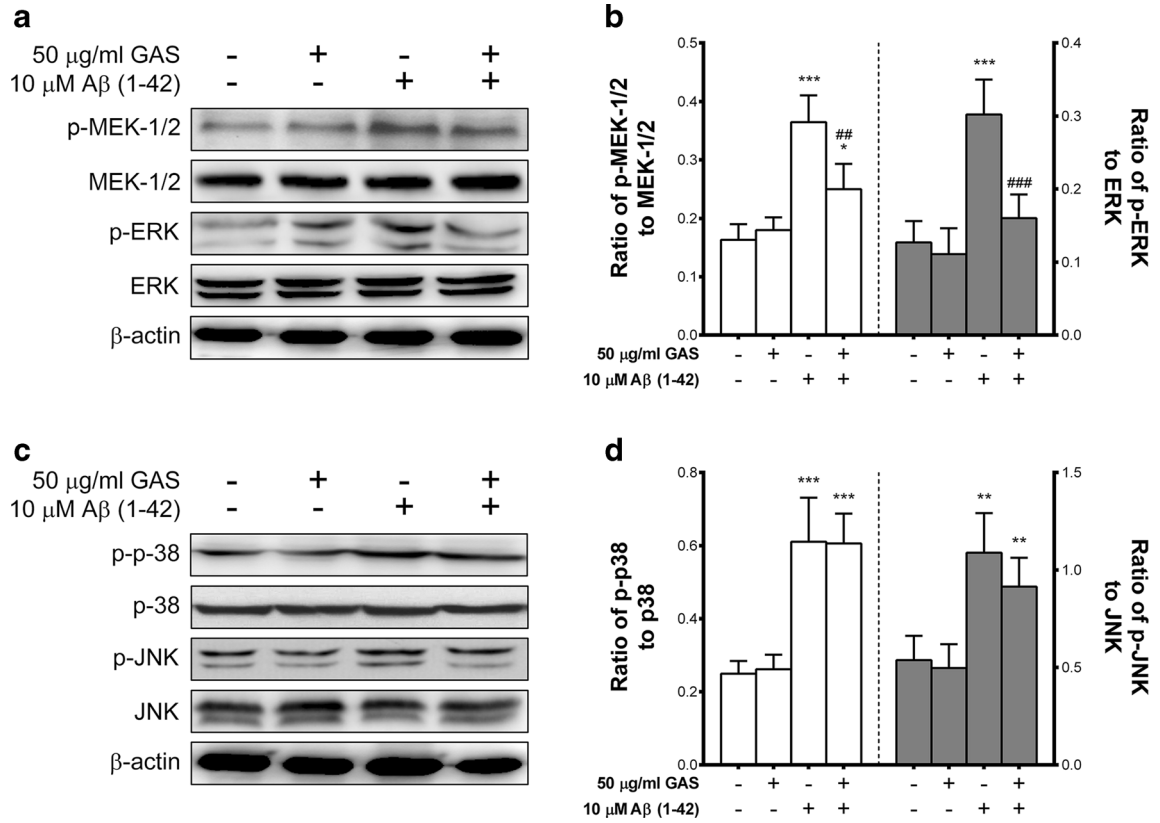

Fig. 6 GAS suppresses Aβ (1–42)-induced activation of the MAPK pathway. NPCs were preincubated with 50 μg/ml of GAS for 6 h prior to Aβ (1–42) treatment for another 2 h. Expression levels of phosphorylated MEK-1/2, ERK, p38, and JNK were detected by Western blot (**a**, **c**) and quantified with ImageJ software (**b**, **d**). All data were from three independent experiments and are presented as mean ± SD. $^{*}P < 0.05$, $^{**}P < 0.01$, and $^{***}P < 0.001$, as compared with the vehicle group; $^{\#\#}P < 0.01$, and $^{\#\#\#}P < 0.001$, as compared with the group treated with Aβ (1–42) alone

life (Zhao et al. 2008). This process is influenced and regulated by a variety of physiological activities, of which the proliferation, differentiation, and fate determination of NPCs are considered greatly essential (Gage 2000). Due to the stem cell properties, adult NPCs can self-renew and differentiate into various neural cells, including neurons, astrocytes, and oligodendrocytes, which are responsible for processing and transmitting information, as well as supporting neuronal function, respectively (Zhao et al., 2008). Nevertheless, in AD, adult neurogenesis is impaired, mainly by the impacts of Aβ on survival and differentiation of NPCs (Crews and Masliah 2010; Curtis et al. 2012; Khan and Berti 2009; Lazarov and Marr 2010). Several lines of evidence have demonstrated that these impacts may be related to Aβ-induced oxidative stress and inflammatory responses, which result in the release of pro-inflammatory cytokines and trigger cell apoptosis (Thal et al. 2015). For example, previous study reported that treatment with Aβ (1–42) could decrease neurosphere proliferation of NPCs and that this process was regulated by an oxidative stress-responsive transcription factor Nrf2 (Karkkainen et al. 2014). In addition, Aβ precursor protein has been found to be able to impair neuronal differentiation of NPCs and induce glial differentiation by activation of the inflammation-associated signaling pathway (Kwak et al. 2010; Shruster et al. 2011). Consistently, our data also showed the toxicity of Aβ (1–42) toward NPCs, which led to decreased cell viability, increased release of pro-inflammatory cytokines and NO, as well as cell apoptosis. Based on these findings, anti-inflammatory and anti-apoptotic interventions may be a natural way to overcome the neurotoxic effects of Aβ and minimize cell damage in NPCs.

In the current study, in vitro experiments revealed that GAS could counteract cell viability loss, inflammatory responses, and cell apoptosis in NPCs following Aβ (1–42) treatment. As the major bioactive component in Tian Ma, GAS has been documented to have potent anti-oxidative, anti-inflammatory, and anti-apoptotic properties both in vitro and in vivo. Peng et al. (2015) reported that in a mice ischemic stroke model, GAS alleviates cerebral ischemic damage through oxidative stress- and inflammation-mediated signaling cascades, whereas Li and Zhang (2015) revealed that GAS improves cognitive dysfunction and decreases oxidative stress in vascular dementia rats induced by chronic ischemia. In a recently published study, GAS was found to ameliorate depression-like behaviors in rats and up-regulate proliferation of hippocampal-derived neural stem

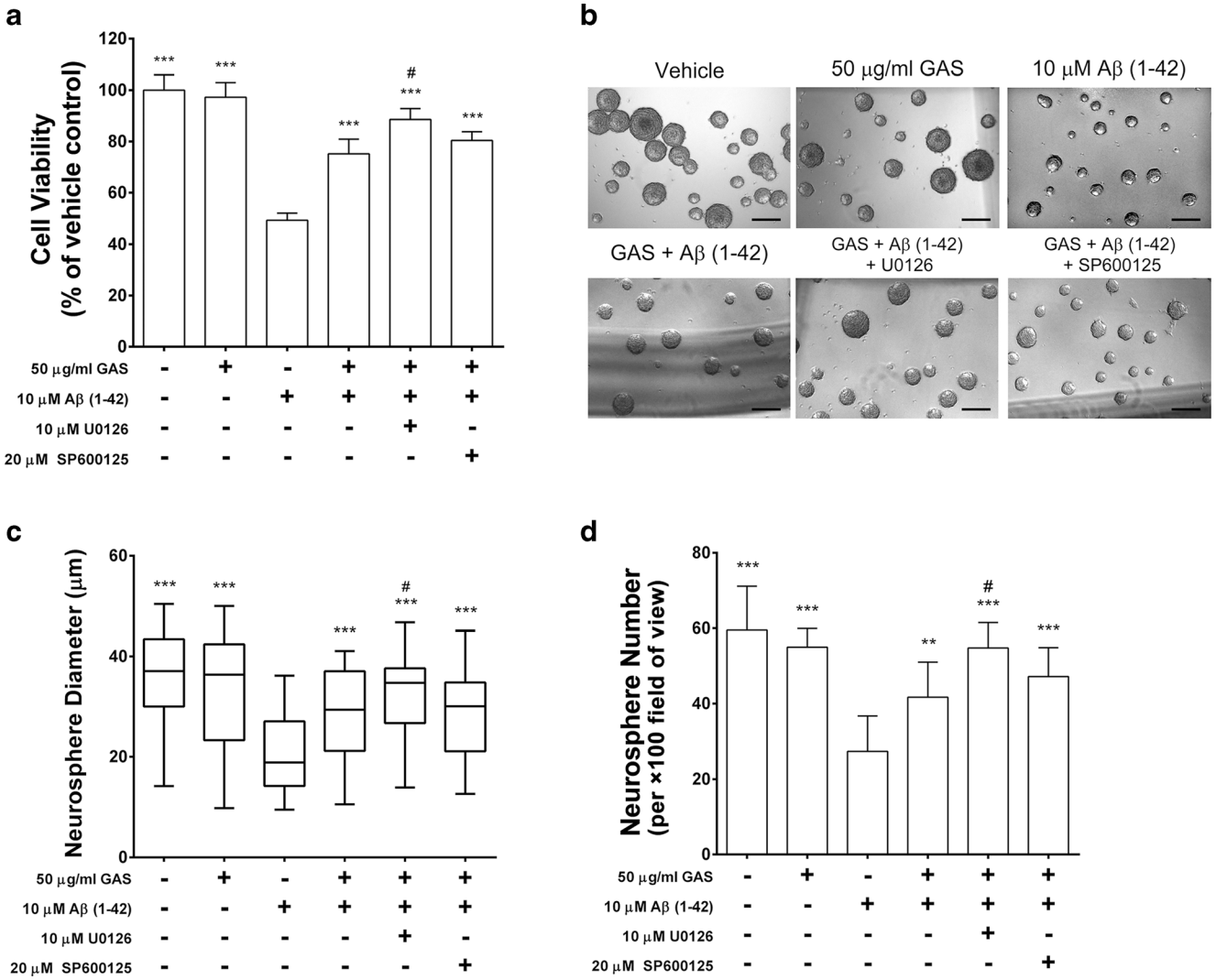

Fig. 7 GAS protects NPCs against Aβ (1–42)-induced neurotoxicity through the MAPK pathway. The MEK inhibitor U0126 (10 μM) or the JNK inhibitor SP600125 (20 μM) were used to treat NPCs for 6 h prior to 50 μg/ml GAS and 10 μM oligomeric Aβ (1–42) treatments. **a** Cell viability after the indicated treatments for 96 h. **b** The morphological appearances of NPCs under the indicated treatment conditions (*scale bar* = 50 μm). **c**, **d** Analysis of neurosphere size and number under the indicated treatment conditions. Cell viability assay was performed in sextuplicate using CCK-8 kit and repeated three times, and the results are presented as mean ± SEM. Neurosphere size analysis was performed in 100 randomly selected neurospheres from 10 random fields of view (200×), and the results are presented as median (*middle line*) and range (*outer lines*). Neurosphere number analysis was performed by calculating the mean neurosphere number of 10 randomly selected 100× fields of view, and the results are presented as mean ± SD. $^{**}P < 0.01$ and $^{***}P < 0.001$, as compared with the group treated with Aβ (1–42) alone; $^{\#}P < 0.05$, as compared with the group treated with Aβ (1–42) plus GAS

cells, in which its anti-inflammatory action was functionally involved (Wang et al. 2014). These published results are in line with the findings obtained in this study. More strikingly, in Aβ (1–42)-injected C57BL/6 mice, we observed that systemic administration of GAS was able to restore the impaired hippocampal neurogenesis caused by Aβ (1–42), which was evidenced by the increased number of SOX-2 and DCX-positive cells in the DG area. Taken together, our data demonstrate the neuroprotective effects of GAS against Aβ (1–42)-induced toxicity. Further mechanistic study indicated that blocking of the activated MAPK signaling cascade by Aβ (1–42) may be an underlying mechanism.

It has been well proven in literature that the activation of the MAPK cascade by Aβ is one of the dominant in vitro and in vivo mechanisms related to AD (Dineley et al. 2001). Soluble and aggregated Aβ can interact with α7 nicotinic acetylcholine receptors (nAChRs), consequently transmitting signals downstream to activate the primary effectors of the MAPK pathway, such as ERK, p38, and JNK, by phosphorylation. These activated molecules, combined with Aβ-induced oxidative stress, mediate pro-inflammatory cytokine expression and promote cell apoptosis, ultimately resulting in the function loss of neuronal cells (Dineley et al. 2001; Rapoport and Ferreira 2000). For GAS, however, several

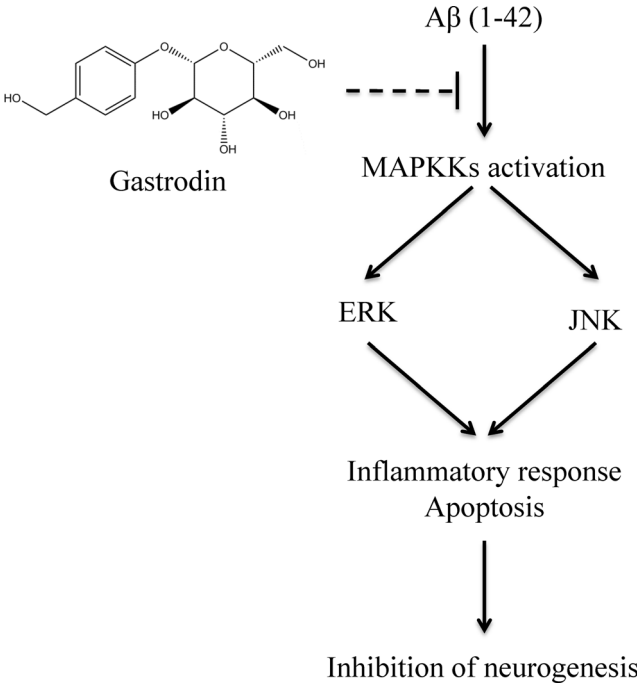

Fig. 8 Molecular mechanism for the neuroprotective effects of GAS against Aβ (1–42)-induced toxicity

studies have demonstrated that its anti-oxidative, anti-inflammatory, and anti-apoptotic effects are exerted mainly via the inhibition of the MAPK signaling cascade. For instance, Dai et al. (2011) found that GAS dramatically decreases expression levels of neurotoxic pro-inflammatory mediators and cytokines through inhibiting the phosphorylation of MAPK signaling effectors in LPS-stimulated microglial cells, while Zhang et al. (2016) reported that GAS alleviates memory deficits in mice via the inhibition of PKR kinase, which is required for p38 MAPK activation. In another in vitro study, GAS attenuates glutamate-induced apoptosis in PC12 cells via blocking the p38 MAPK/p53 signaling cascade (Jiang et al. 2014). In line with these reports, Western blot analysis of the present study showed elevated phosphorylation of MEK, ERK, and JNK in Aβ (1–42)-treated NPCs, but this Aβ-induced effect could be reversed by preincubation with GAS. Additionally, the combination of GAS either with MEK inhibitor U0126 or with JNK inhibitor SP600125 was able to synergistically counteract Aβ (1–42)-induced decrease in cell viability and growth. Taken collectively, these data provide direct evidence on the important role of MAPK pathway inhibition as the key mechanism involved in the neuroprotective effects of GAS against Aβ.

An interesting finding in our study was that GAS alone neither directly stimulates survival and proliferation of cultured NPCs, nor directly increases the number of SOX-2 and DCX-positive cells in the DG area of the adult mouse brain. These results were consistent with the previous study by Wang et al. (2014). In addition, treatment with GAS alone could not counteract Aβ (1–42)-induced increase in the phosphorylation of MAPKs. Therefore, we speculate that GAS might be a molecule that can interfere with the interaction between Aβ (1–42) and nAChRs and/or other putative cellular receptors. Moreover, previous literature has shown that GAS can improve memory and cognitive impairment in 3, 3′-iminodipropionitrile-treated mice (Wang et al. 2016; 2015b), which leads to a speculation that GAS may ameliorate Aβ-induced memory and cognitive impairment. However, further studies are required to obtain solid evidence supporting these speculations.

In summary, this study reveals that GAS is able to protect cultured primary NPCs against Aβ (1–42)-induced neurotoxicity and improve hippocampal neurogenesis in Aβ (1–42)-injected C57BL/6 mice. Mechanistic studies suggest that the MAPK signaling cascade is involved in mediating the neuroprotective effects of GAS (the hypothetical scheme is shown in Fig. 8). These findings provide substantial insight into the potential merits of GAS for its clinical application in the treatment of AD.

Acknowledgments All authors would like to thank Dr. Zhenhuan Zheng for his kind assistance in data analysis and preparation of the manuscript.

Compliance with Ethical Standards

Conflict of Interest The authors declare that they have no conflict of interest.

References

Apetz N, Munch G, Govindaraghavan S, Gyengesi E (2014) Natural compounds and plant extracts as therapeutics against chronic inflammation in Alzheimer's disease–a translational perspective. CNS Neurol Disord Drug Targets 13(7):1175–1191

Burns A, Iliffe S (2009) Alzheimer's disease. BMJ 338:b158

Chen PZ, Jiang HH, Wen B, Ren SC, Chen Y, Ji WG, et al. (2014) Gastrodin suppresses the amyloid beta-induced increase of spontaneous discharge in the entorhinal cortex of rats. Neural Plast 2014: 320937

Crews L, Masliah E (2010) Molecular mechanisms of neurodegeneration in Alzheimer's disease. Hum Mol Genet 19(R1):R12–R20

Curtis MA, Low VF, Faull RL (2012) Neurogenesis and progenitor cells in the adult human brain: a comparison between hippocampal and subventricular progenitor proliferation. Dev Neurobiol 72(7):990–1005

Dai JN, Zong Y, Zhong LM, Li YM, Zhang W, Bian LG, et al. (2011) Gastrodin inhibits expression of inducible NO synthase, cyclooxygenase-2 and proinflammatory cytokines in cultured LPS-stimulated microglia via MAPK pathways. PLoS One 6(7):e21891

Dawkins E, Small DH (2014) Insights into the physiological function of the beta-amyloid precursor protein: beyond Alzheimer's disease. J Neurochem 129(5):756–769

Dineley KT, Westerman M, Bui D, Bell K, Ashe KH, Sweatt JD (2001) Beta-amyloid activates the mitogen-activated protein kinase cascade via hippocampal alpha7 nicotinic acetylcholine receptors: in vitro

and in vivo mechanisms related to Alzheimer's disease. J Neurosci 21(12):4125–4133
Eriksson PS, Perfilieva E, Bjork-Eriksson T, Alborn AM, Nordborg C, Peterson DA, et al. (1998) Neurogenesis in the adult human hippocampus. Nat Med 4(11):1313–1317
Fuster-Matanzo A, Llorens-Martin M, Hernandez F, Avila J (2013) Role of neuroinflammation in adult neurogenesis and Alzheimer disease: therapeutic approaches. Mediat Inflamm 2013:260925
Gage FH (2000) Mammalian neural stem cells. Science 287(5457):1433–1438
He N, Jin WL, Lok KH, Wang Y, Yin M, Wang ZJ (2013) Amyloid-beta(1-42) oligomer accelerates senescence in adult hippocampal neural stem/progenitor cells via formylpeptide receptor 2. Cell Death Dis 4:e924
Hou Y, Ghosh P, Wan R, Ouyang X, Cheng H, Mattson MP, et al. (2014) Permeability transition pore-mediated mitochondrial superoxide flashes mediate an early inhibitory effect of amyloid beta1-42 on neural progenitor cell proliferation. Neurobiol Aging 35(5):975–989
Hu Y, Li C, Shen W (2014) Gastrodin alleviates memory deficits and reduces neuropathology in a mouse model of Alzheimer's disease. Neuropathology 34(4):370–377
Jang JH, Son Y, Kang SS, Bae CS, Kim JC, Kim SH, et al. (2015) Neuropharmacological potential of Gastrodia elata Blume and its components. Evid Based Complement Alternat Med 2015:309261
Jiang G, Wu H, Hu Y, Li J, Li Q (2014) Gastrodin inhibits glutamate-induced apoptosis of PC12 cells via inhibition of CaMKII/ASK-1/p38 MAPK/p53 signaling cascade. Cell Mol Neurobiol 34(4):591–602
Karkkainen V, Pomeshchik Y, Savchenko E, Dhungana H, Kurronen A, Lehtonen S, et al. (2014) Nrf2 regulates neurogenesis and protects neural progenitor cells against Abeta toxicity. Stem Cells 32(7):1904–1916
Khan MA, Berti L (2009) Alzheimer's disease affects progenitor cells through aberrant {beta}-catenin signaling. J Neurosci 29(40):12369–12371
Kwak YD, Dantuma E, Merchant S, Bushnev S, Sugaya K (2010) Amyloid-beta precursor protein induces glial differentiation of neural progenitor cells by activation of the IL-6/gp130 signaling pathway. Neurotox Res 18(3–4):328–338
Lazarov O, Marr RA (2010) Neurogenesis and Alzheimer's disease: at the crossroads. Exp Neurol 223(2):267–281
Li Y, Zhang Z (2015) Gastrodin improves cognitive dysfunction and decreases oxidative stress in vascular dementia rats induced by chronic ischemia. Int J Clin Exp Pathol 8(11):14099–14109
Martino G, Butti E, Bacigaluppi M (2014) Neurogenesis or non-neurogenesis: that is the question. J Clin Invest 124(3):970–973
Minter MR, Taylor JM, Crack PJ (2016) The contribution of neuroinflammation to amyloid toxicity in Alzheimer's disease. J Neurochem 136(3):457–474
Origlia N, Arancio O, Domenici L, Yan SS (2009) MAPK, beta-amyloid and synaptic dysfunction: the role of RAGE. Expert Rev Neurother 9(11):1635–1645
Peng Z, Wang S, Chen G, Cai M, Liu R, Deng J, et al. (2015) Gastrodin alleviates cerebral ischemic damage in mice by improving anti-oxidant and anti-inflammation activities and inhibiting apoptosis pathway. Neurochem Res 40(4):661–673
Qu LL, Yu B, Li Z, Jiang WX, Jiang JD, Kong WJ (2015) Gastrodin ameliorates oxidative stress and proinflammatory response in non-alcoholic fatty liver disease through the AMPK/Nrf2 pathway. Phytother Res 30(3):402–411
Rapoport M, Ferreira A (2000) PD98059 prevents neurite degeneration induced by fibrillar beta-amyloid in mature hippocampal neurons. J Neurochem 74(1):125–133
Sanphui P, Biswas SC (2013) FoxO3a is activated and executes neuron death via Bim in response to beta-amyloid. Cell Death Dis 4:e625
Schmittgen TD, Livak KJ (2008) Analyzing real-time PCR data by the comparative C(T) method. Nat Protoc 3(6):1101–1108
Shruster A, Eldar-Finkelman H, Melamed E, Offen D (2011) Wnt signaling pathway overcomes the disruption of neuronal differentiation of neural progenitor cells induced by oligomeric amyloid beta-peptide. J Neurochem 116(4):522–529
Smith LK, He Y, Park JS, Bieri G, Snethlage CE, Lin K, et al. (2015) beta2-microglobulin is a systemic pro-aging factor that impairs cognitive function and neurogenesis. Nat Med 21(8):932–937
Sun G, Yuan Z, Zhang B, Jia Y, Ji Y, Ma X, et al. (2012) Gastrodin blocks neural stem cell differentiation into glial cells mediated by kainic acid. Neural Regen Res 7(12):891–895
Thal DR, Walter J, Saido TC, Fandrich M (2015) Neuropathology and biochemistry of Abeta and its aggregates in Alzheimer's disease. Acta Neuropathol 129(2):167–182
Wang H, Zhang R, Qiao Y, Xue F, Nie H, Zhang Z, et al. (2014) Gastrodin ameliorates depression-like behaviors and up-regulates proliferation of hippocampal-derived neural stem cells in rats: involvement of its anti-inflammatory action. Behav Brain Res 266:153–160
Wang J, Tan L, Wang HF, Tan CC, Meng XF, Wang C, et al. (2015a) Anti-inflammatory drugs and risk of Alzheimer's disease: an updated systematic review and meta-analysis. J Alzheimers Dis 44(2):385–396
Wang X, Li P, Liu J, Jin X, Li L, Zhang D, et al. (2016) Gastrodin attenuates cognitive deficits induced by 3,3′-iminodipropionitrile . doi:10.1007/s11064-016-1845-9Neurochem Res
Wang X, Tan Y, Zhang F (2015b) Ameliorative effect of gastrodin on 3,3′-iminodipropionitrile-induced memory impairment in rats. Neurosci Lett 594:40–45
Winner B, Winkler J (2015) Adult neurogenesis in neurodegenerative diseases. Cold Spring Harb Perspect Biol 7(4):a021287
Wu C, Fujihara H, Yao J, Qi S, Li H, Shimoji K, et al. (2003) Different expression patterns of Bcl-2, Bcl-xl, and Bax proteins after sublethal forebrain ischemia in C57Black/Crj6 mouse striatum. Stroke 34(7):1803–1808
Yang P, Han Y, Gui L, Sun J, Chen YL, Song R, et al. (2013) Gastrodin attenuation of the inflammatory response in H9c2 cardiomyocytes involves inhibition of NF-kappaB and MAPKs activation via the phosphatidylinositol 3-kinase signaling. Biochem Pharmacol 85(8):1124–1133
Zhang JS, Zhou SF, Wang Q, Guo JN, Liang HM, Deng JB, et al. (2016) Gastrodin suppresses BACE1 expression under oxidative stress condition via inhibition of the PKR/eIF2alpha pathway in Alzheimer's disease. Neuroscience pii S0306-4522(16):00247–00245. doi:10.1016/j.neuroscience.2016.03.024
Zhao C, Deng W, Gage FH (2008) Mechanisms and functional implications of adult neurogenesis. Cell 132(4):645–660
Zhao H, Wang SL, Qian L, Jin JL, Li H, Xu Y, et al. (2013) Diammonium glycyrrhizinate attenuates Abeta(1-42)-induced neuroinflammation and regulates MAPK and NF-kappaB pathways in vitro and in vivo. CNS Neurosci Ther 19(2):117–124
Zhao X, Zou Y, Xu H, Fan L, Guo H, Li X, et al. (2012) Gastrodin protect primary cultured rat hippocampal neurons against amyloid-beta peptide-induced neurotoxicity via ERK1/2-Nrf2 pathway. Brain Res 1482:13–21